Solvent effects on the vibronic one-photon absorption profiles of dioxaborine heterocycles

Yan-Hua Wang, Marcus Halik, Chuan-Kui Wang, Seth R. Marder, and Yi Luo

Citation: J. Chem. Phys. **123**, 194311 (2005); doi: 10.1063/1.2121590
View online: http://dx.doi.org/10.1063/1.2121590
View Table of Contents: http://jcp.aip.org/resource/1/JCPSA6/v123/i19
Published by the American Institute of Physics.

Solvent effects on the vibronic one-photon absorption profiles of dioxaborine heterocycles

Yan-Hua Wang
Department of Theoretical Chemistry, Royal Institute of Technology, AlbaNova University Center, S-106 91 Stockholm, Sweden and College of Physics and Electronics, Shandong Normal University, 250014 Jinan, Shandong, People's Republic of China

Marcus Halik
Department of Chemistry, University of Arizona, Tucson Arizona 85721

Chuan-Kui Wang
Department of Theoretical Chemistry, Royal Institute of Technology, AlbaNova University Center, S-106 91 Stockholm, Sweden and College of Physics and Electronics, Shandong Normal University, 250014 Jinan, Shandong, People's Republic of China

Seth R. Marder
Department of Chemistry, University of Arizona, Tucson Arizona 85721 and School of Chemistry and Biochemistry, Georgia Institute of Technology, Atlanta, Georgia 30332

Yi Luo[a)]
Department of Theoretical Chemistry, Royal Institute of Technology, AlbaNova University Center, S-106 91 Stockholm, Sweden

(Received 23 June 2005; accepted 21 September 2005; published online 17 November 2005)

The vibronic profiles of one-photon absorption spectra of dioxaborine heterocycles in gas phase and solution have been calculated at the Hartree-Fock and density-functional-theory levels. The polarizable continuum model has been applied to simulate the solvent effect, while the linear coupling model is used to compute the Franck-Condon and Herzberg-Teller contributions. It is found that a good agreement between theory and experiment can be achieved when the solvent effect and electron correlation are taken into account simultaneously. For the first excited charge-transfer state, the maximum of its Herzberg-Teller profile is blueshifted from that of the Franck-Condon profile. The shifted energy is found to be around 0.2 eV, which agrees well with the measured energy difference between two- and one-photon absorptions of the first excited state. © *2005 American Institute of Physics*. [DOI: 10.1063/1.2121590]

I. INTRODUCTION

Charge-transfer organic molecules have attracted considerable attention owing to their excellent characteristics, such as large third-order nonlinearities, instantaneous response times, high damage thresholds, ease of processing and structural modification, and their applicability over a wide range of wavelengths. Recently, it was found that symmetric charge transfer from the ends to the middle of the conjugated systems with donor-acceptor-donor or acceptor-donor-acceptor arrangements can give rise to large two-photon absorption cross sections.[1–4] Two-photon technology has become increasingly important for many applications. Design and characterization of new chromophores with even larger two-photon absorption cross section have been the main theme of recent theoretical and experimental studies.[5,6] However, among many techniques, one-photon absorption has always been used as the primary tool to characterize the compounds.

There are two important aspects that should be considered in the modeling of the one-photon absorption spectra of molecules. One is the influence of the solvent on the electronic and geometrical structures of the charge-transfer complexes since almost all experimental measurements for charge-transfer organic molecules are carried out in the liquid phase or in solutions. Over the years, many experimental[7–9] and theoretical[10–12] studies have been devoted to understand these effects. Another issue is related to the spectral profile of the one-photon absorption spectrum. The experimental absorption spectra are often vibrationally resolved and the inclusion of vibronic coupling in the modeling of the spectra becomes essential. A relatively simple linear coupling model (LCM) has been shown to be very useful for many cases.[13–16] Recently, Dierksen and Grimme[15] have calculated the vibronic structures in the electronic spectra of a series of organic molecules based on density-functional-theory (DFT) methods. In this work, we have combined several computational approaches to take into account the solvent effects and vibronic coupling simultaneously. We have used Hartree-Fock (HF) and DFT methods for the electronic and geometrical structures, time-dependent (TD) HF and TDDFT for the optical excitations, LCM for the vibronic couplings, and polarizable continuum model (PCM) for the solvent effects.

[a)]Author to whom correspondence should be addressed. Electronic mail: luo@theochem.kth.se

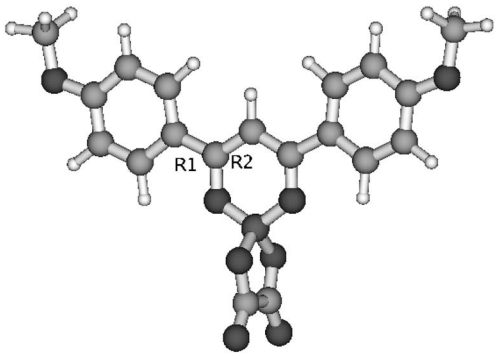

FIG. 1. Structure of compound 1 in DCM solution optimized with the B3LYP/PCM method.

The molecular systems used in the calculations are dioxaborine heterocycles which are 1:1 chelate complexes formed from enolizable 1,3-diketones and boronic acid derivatives or halogens. The boron atom fixes a negative charge so the π system of the dicarbonyl ligands is positively charged, making the group a strong acceptor as evidenced by a high electron affinity.[17] In addition the chromophore containing this acceptor tends to have strong absorption bands,[18] high thermal stability, and, in contrast to complexes with heavy metal ions, a strong fluorescence in solution and in the solid state.[19] In this study we examine the synthesis of compound 1 (as given in Fig. 1) according to the procedures described previously.[20] The compound was obtained in 40% yield and UV/visible (VIS) had a λ_{max} in CH_2Cl_2 at 431 nm with a molar absorptivity $\epsilon = 57.500\ \mathrm{l\ mol^{-1}\ cm^{-1}}$.

II. COMPUTATIONAL METHOD

For one-photon absorption, the transition probability can be evaluated by the oscillator strength which is calculated from

$$W_{if} = \frac{2}{3}\omega_{if}\mu_{if}^2, \tag{1}$$

where ω_{if} is the transition energy and $\mu_{if} = \langle i|\mu|f\rangle$ is the transition electric dipole moment from the initial state i to the final state f. If one takes into account both electronic and vibrational states, the transition electric dipole moment can be expressed explicitly as

$$\mu_{g\upsilon eu} = \langle g\upsilon|\mu|eu\rangle, \tag{2}$$

where υ, u represent the vibrational states of the electronic states g and e, respectively. Applying the Born-Oppenheimer adiabatic approximation to the above formula, one has

$$\mu_{g\upsilon eu} = \langle \upsilon|\mu_{ge}^e(Q)|u\rangle, \tag{3}$$

where $\mu_{ge}^e(Q)$ is the electronic part of the transition dipole moment, which can be expanded in the normal modes:

$$\mu_{ge}(Q) = \mu_{ge}^e(Q)_0 + \sum_a \frac{\partial \mu_{ge}^e}{\partial Q_a} Q_a + \ldots . \tag{4}$$

If taking only the first two terms of the expansion into account and submitting them into Eq. (3), one will get

$$\mu_{g\upsilon eu} = \mu_{ge}^e(Q)_0\langle \upsilon|u\rangle + \sum_a \frac{\partial \mu_{ge}^e}{\partial Q_a}\langle \upsilon|Q_a|u\rangle. \tag{5}$$

Here the first and second terms give the Franck-Condon (FC) and Herzberg-Teller (HT) contributions, respectively, to the one-photon absorption.

In this work, the linear coupling model is applied which assumes that both excited and ground electronic states have the same harmonic potential-energy surface curvatures but are mutually displaced. The displacement d_a of a normal mode a in the excited-state potential-energy surface is possible to be obtained from the gradient G_a of the excited-state energy E^{S_1},[16]

$$d_a = \frac{G_a}{\omega_a^2}, \quad G_a = \frac{\partial E^{S_1}}{\partial Q_a}, \tag{6}$$

where ω_a is the vibrational frequency of normal mode a.

For a normal mode a, a general expression for the overlap between two displaced vibronic states with occupation numbers $m_a \leqslant n_a$ can be written as

$$\langle m_a|n_a\rangle = (-1)^{n_a-m_a}e^{-x/2}x^{(n_a-m_a)/2}\sqrt{\frac{m_a!}{n_a!}}L_{m_a}^{n_a-m_a}(x), \tag{7}$$

where x is a dimensionless parameter depending on the displacement d_a and the vibrational frequency ω_a as $x = \omega_a d_a^2/2\hbar$. $L_{n_a}^{m_a-n_a}(x)$ is the associated Laguerre polynomial,

$$L_{m_a}^{n_a-m_a}(x) = \sum_{r=0}^{m_a}\frac{n_a!(-x)^r}{(m_a-r)!(n_a-m_a+r)!r!}. \tag{8}$$

For $m_a > n_a$, we have $\langle m_a|n_a\rangle = (-1)^{m_a-n_a}\langle n_a|m_a\rangle$.

The element $\langle m_a|Q_a|n_a\rangle$ can be easily connected with the element $\langle m_a|n_a\rangle$ by using the raising and lowering operators of the initial harmonic oscillator,[16]

$$Q_a = \sqrt{\frac{\hbar}{2\omega_a}}(a^\dagger + a), \tag{9}$$

$$\langle m_a|Q_a|n_a\rangle = \sqrt{\frac{\hbar}{2\omega_a}}(\sqrt{m_a+1}\langle m_a+1|n_a\rangle + \sqrt{m_a}\langle m_a-1|n_a\rangle). \tag{10}$$

For a multimode situation, we need to evaluate the product of the single displaced harmonic-oscillator overlap integrals,

$$\langle \upsilon|u\rangle = \prod_a \langle m_a^\upsilon|n_a^u\rangle, \tag{11}$$

$$\langle \upsilon|Q_a|u\rangle = \langle m_a^\upsilon|Q_a|n_a^u\rangle\prod_{b\neq a}\langle m_b^\upsilon|n_b^u\rangle. \tag{12}$$

The transition dipole moment has finally the form,

TABLE I. The electronic states of compound 1 calculated at different theoretical levels: the excitation energy (E_{eg} in eV), the corresponding wavelength (λ_{eg} in nm), the oscillator strength (osc), and the radiative lifetime (τ in ns). Different optimized geometries have been used for different time-dependent methods. The DCM solution is used in the PCM calculations.

		Excited state 1				Excited state 2			
TD Method	Geometry	E_{eg}	λ_{eg}	osc.	τ	E_{eg}	λ_{eg}	osc.	τ
HF	AM1	4.29	288.87	1.16	1.08	4.81	257.51	0.00	···
HF	HF	4.44	279.45	1.20	0.98	5.36	231.38	0.00	···
HF	B3LYP	4.28	289.75	1.21	1.04	5.12	241.95	0.00	···
B3LYP	AM1	3.12	396.89	0.00	···	3.28	378.31	0.95	2.26
B3LYP	HF	3.02	409.97	0.00	···	3.39	365.27	1.01	1.98
B3LYP	B3LYP	3.02	409.96	0.00	···	3.30	376.05	1.02	2.08
B3LYP	B3LYP/PCM	2.68	462.82	0.00	···	3.24	382.40	1.01	2.17
BP86	BP86	1.73	717.01	0.00	···	2.64	468.92	0.02	164.83
BLYP	BLYP	1.74	711.44	0.00	···	2.65	468.26	0.03	109.58
HF/PCM	HF/PCM	4.16	298.01	1.39	0.96	5.34	232.16	0.28	2.89
HF/PCM	B3LYP/PCM	3.99	310.48	1.40	1.03	5.22	237.46	0.29	2.92
B3LYP/PCM	HF/PCM	3.14	395.03	1.20	1.95	3.82	324.49	0.18	8.77
B3LYP/PCM	B3LYP/PCM	3.04	407.74	1.22	2.04	3.74	331.49	0.19	8.67

$$\mu_{gveu} = \mu^e_{ge}(Q)_0 \prod_a \langle m^v_a | n^u_a \rangle + \sum_a \frac{\partial \mu^e_{ge}}{\partial Q_a} \langle m^v_a | Q_a | n^u_a \rangle \prod_{b \neq a} \langle m^v_b | n^u_b \rangle. \tag{13}$$

In this work, the vibronic profiles of the one-photon absorption spectrum of compound 1 in dichloromethane (DCM) solvent are calculated using the HF and DFT methods together with the integral equation formalism polarizable continuum model (IEF-PCM).[21]

It should be noted that the excited-state geometries can be optimized with various computational methods, for instance, the configuration interaction singles (CIS) (Ref. 22) approach. With the knowledge of both ground- and excited-state geometries, the displacement d_a of normal mode a can be computed analytically[23]

$$d_a = (\mathbf{x_f} - \mathbf{x_i})\mathbf{M}^{1/2}\mathbf{L_{a,f}}, \tag{14}$$

where $\mathbf{x_i}$ and $\mathbf{x_f}$ are the $3N$-dimensional vectors of the equilibrium Cartesian coordinates in states i and f and $\mathbf{M}$ is the $3N \times 3N$ diagonal matrix of the atomic masses. $\mathbf{L_{a,f}}$ is the $3N$ vector of the normal coordinates of the vibrational mode a in terms of mass-weighted Cartesian coordinates.

Previous studies[13,14,24] have shown that CIS combining with TDHF often gives reasonable results. We have employed RCIS/6–31G* method to optimize the first excited state of the molecule under investigation. Unfortunately, the results for compound 1 are found to be in complete disagreement with the experimental spectrum. As we will discuss later, the electronic structures of compound 1 are very sensitive to the computational methods applied.

The molecular geometries at the ground state are optimized with the semiempirical method Austin Model 1 (AM1) (Ref. 25) and the HF and DFT methods, respectively. The gradient-corrected DFT methods with BP86 (Refs. 26 and 27) and BLYP (Refs. 26 and 28) functionals, as well as the hybrid functional B3LYP,[28,29] are applied. The excitation energies of the lowest singlet excited states are calculated using the TDHF and TDDFT methods at the optimized geometries of different theoretical levels. A summary of different combinations examined in this work can be found in Table I. The gradient G_a of the excitation energy E^{S_1} is calculated numerically. The basis set 6–31G* (Ref. 30) is used for all the quantum-chemical calculations, which are performed with the GAUSSIAN 03 program.[31]

III. RESULTS AND DISCUSSION

The molecular structure optimized by the DFT/3LYP-PCM method in DCM solvent is shown in Fig. 1. The lengths of the single C–C bond $R1$ and the double C=C bond $R2$ are 1.458 and 1.396 Å, respectively, with a bond length alternation (BLA) of 0.062 Å. The BLA calculated with BP86, BLYP, and B3LYP without considering the solvent effect are found to be 0.064, 0.066, and 0.068 Å, respectively, while the HF and HF-PCM give values of 0.078 and 0.074 Å, respectively. It is noted that the inclusion of DCM solvent and electron correlation reduces the BLA value. In general, the difference in BLA values obtained from different DFT methods is quite small.

The excitation energies, oscillator strengths, and radiative lifetimes of the first two excited states calculated with different geometries are listed in Table I. Within the HF, the first excited state (S_1) is a strong one-photon absorption state, i.e., a typical charge-transfer state, while the second state (S_2) has a much smaller oscillator strength. The excitation energy to S_1 state is found to be around 4.4 eV for all geometries. It is much larger than the experimental absorption maximum of the first band, around 2.90 eV.

It is expected that the inclusion of electron correlation should improve the calculated excitation energies. Indeed, the TD-B3LYP calculations at geometries optimized at AM1, HF, and B3LYP levels give a value of 3.12–3.02 eV for the S_1 state, very close to the experimental result. However, the character of the S_1 state from the B3LYP is different from the HF; its oscillator strength is found to be zero. The second state becomes a charge-transfer state with a large oscillator

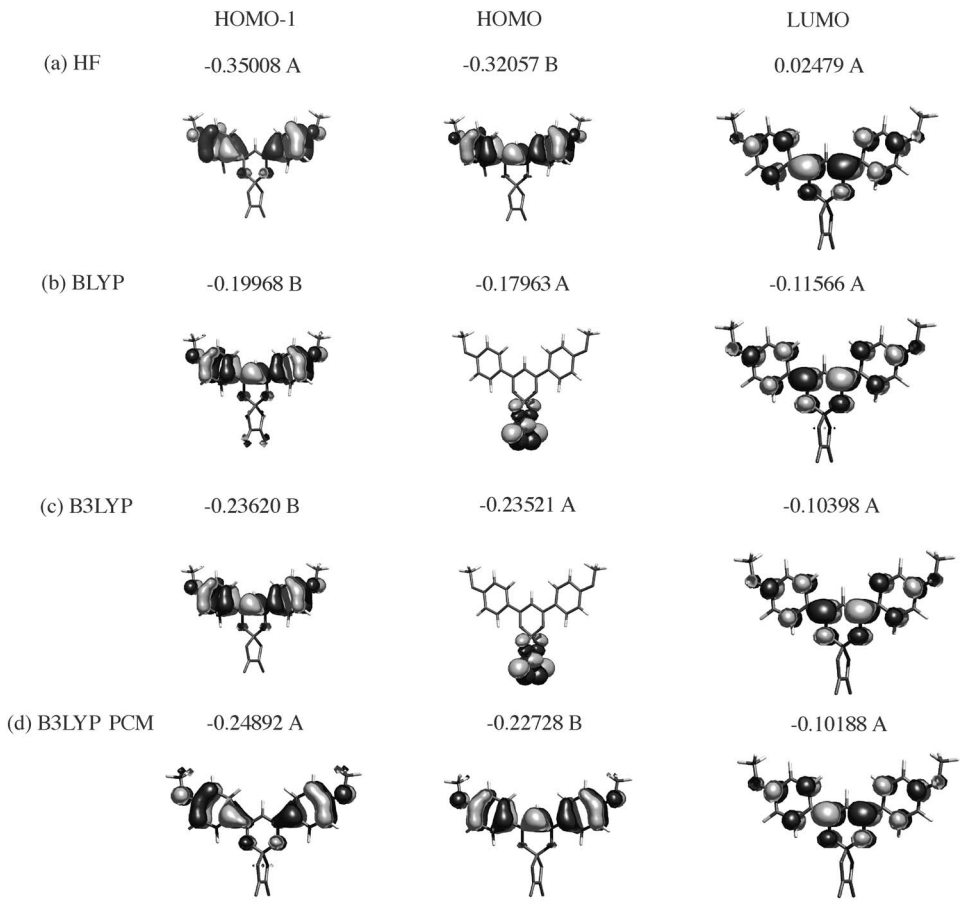

FIG. 2. Molecular orbitals, HOMO-1, HOMO, and LUMO, of compound 1 calculated with different methods on the corresponding optimized geometries: (a) HF, (b) BLYP, (c) B3LYP, and (d) B3LYP/PCM. The digit above each figure is the corresponding orbital energy and the character after the digit is the symmetry of the orbital.

strength. Apparently the B3LYP method has altered the order of the electronic states of compound 1. To understand this finding, we have also carried out the calculations using the gradient-corrected functionals, BP86 and BLYP. The excitation energies of S_1 and S_2 states become even smaller, around 1.73 and 2.64 eV, respectively, both without oscillator strength. With these two functionals, the third excited state becomes the charge-transfer state, whose oscillator strength is found to be 0.8. These DFT methods seem to fail to describe the electronic structures of compound 1 in the gas phase.

We have plotted out the highest occupied molecular orbital (HOMO), HOMO-1, and the lowest unoccupied molecular orbital (LUMO) obtained from HF, BLYP, and B3LYP at the corresponding optimized geometries, shown in Fig. 2 with symmetry assignment. Compound 1 has a symmetry close to the C2 group. It is noted that all methods give the same description for the LUMO (with *A* symmetry), while the character of the HOMO is different between HF (with *B* symmetry) and DFT (with *A* symmetry) methods. The HOMO from DFT calculations is strongly localized outside of the back bond of the molecule, resulting in the zero

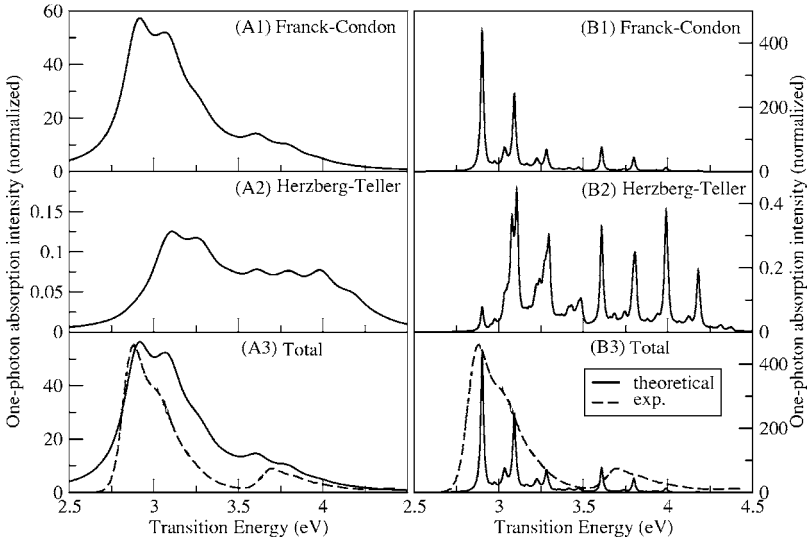

FIG. 3. One-photon absorption spectra of compound 1 in the DCM solution calculated with the TD-B3LYP/PCM method at the B3LYP/PCM geometry. The Franck-Condon contribution (A1, B1), the Herzberg-Teller contribution (A2, B2), and the total spectra (A3, B3) are presented with lifetime broadenings of 0.10 and 0.01 eV, respectively. The experimental spectrum is shown by the dashed lines.

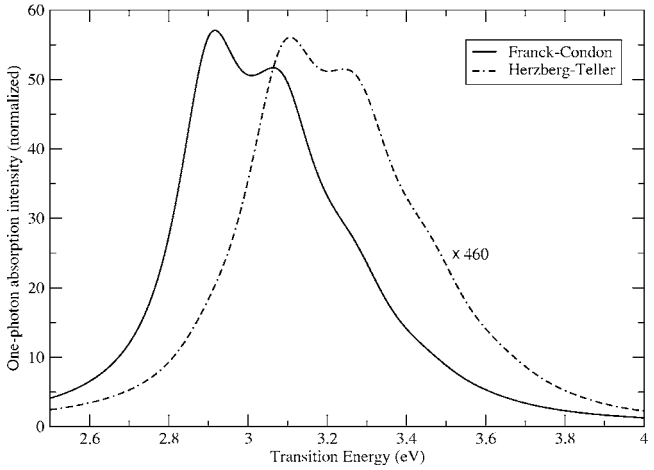

FIG. 4. Franck-Condon (solid line) and Herzberg-Teller (dash-dot-dash line) profiles of the OPA of compound 1 in the DCM solution calculated with the TD-B3LYP/PCM method at the B3LYP/PCM geometry.

transition probability going from HOMO to LUMO. The HOMO-1 from DFT calculations is of symmetry *B*. Furthermore, the BLYP gives very low orbital energies for the HOMO and HOMO-1; consequently, very low excitation energies for S_1 and S_2 states. The charge-transfer state is attributed to the transition between orbitals with symmetry *A* and symmetry *B* and possesses very large oscillator strengths.

It is clear that the calculated results for the gas-phase molecule cannot describe properly the experimental absorption spectrum of compound 1 in DCM solution. The study of the solvent effects has thus become relevant. We have optimized the geometry of compound 1 in DCM using the PCM method at both HF and B3LYP levels. The orbital characters obtained from HF/PCM are very similar to those in the gas phase. However, solvent effects have a strong impact on the molecular orbitals obtained at the B3LYP level. As shown in Fig. 2(d), the HOMO from the B3LYP/PCM calculation becomes a delocalized orbital, similar to what HF has given. The S_1 state becomes a one-photon absorption allowed state. The TD-B3LYP/PCM calculation gives a value of 3.04 eV for the excitation energy of the S_1 state and 3.74 eV for the S_2 state. Both values fit the maxima of the experimental absorption bands. The calculated radiative lifetime is 2.04 ns for S_1 and 8.67 ns for S_2, respectively.

It is obvious that one needs to model the vibronic profiles for the one-photon absorption (OPA) of compound 1 in order to reproduce the experimental spectrum. We have simulated the vibronic profiles for the OPA of compound 1 at different theoretical levels. We start with the B3LYP/PCM calculations and the results are shown in Fig. 3 with two different lifetime broadenings, 0.1 and 0.01 eV, respectively. The calculated total spectrum is found to be in good agreement with the experiment. Due to the vibrational contribution, the maximum of the spectral profile of the first band shifted by −0.14 eV from the calculated vertical transition (from 3.04 to 2.90 eV). The Franck-Condon and Herzberg-Teller contributions to the total spectrum are also presented. It is clear that in the spectral region discussed here, the Franck-Condon contribution plays a dominant role. Nevertheless, it is interesting to see that the maximum of the Herzberg-Teller profile is blueshifted by 0.2 eV, with respect to the maximum of the Franck-Condon profile, as shown in Fig. 4. Such an observation is relevant to the discussion of the two-photon absorption spectral profile. For compound 1, the S_1 state is a strong one-photon absorption state, but a very weak two-photon absorption state. In the case of two-photon absorption (TPA), the Franck-Condon contribution is thus diminished, and the Herzberg-Teller contribution becomes important or even dominate. One can thus anticipate that the maximum of OPA can be different from that of TPA, which is indeed what the experimental OPA and TPA spectra have shown. More studies on the vibronic profiles of TPA of compound 1 are in progress.

In Table II, information about the vibration modes of compound 1 in DCM with noticeable displacements is given.

TABLE II. Frequency, displacement, and Franck-Condon factors of the most important vibrational modes calculated with the B3LYP/PCM method.

Mode	ω_a (cm^{-1})	d (a.u.)	δE (cm^{-1})	$\lvert\langle 0\rvert 0\rangle\rvert^2$	$\lvert\langle 0\rvert 1\rangle\rvert^2$	$\lvert\langle 0\rvert 2\rangle\rvert^2$
29	417	−4	−7	0.98	0.02	0.00
36	588	−5	−19	0.97	0.03	0.00
40	643	−3	−7	0.99	0.01	0.00
43	706	2	−5	0.99	0.01	0.00
52	821	−3	−13	0.98	0.02	0.00
57	905	2	−9	0.99	0.01	0.00
60	966	2	−13	0.99	0.01	0.00
67	1051	3	−26	0.98	0.02	0.00
69	1059	5	−66	0.94	0.06	0.00
70	1123	−5	−62	0.95	0.05	0.00
73	1157	1	−6	0.99	0.01	0.00
79	1218	1	−7	0.99	0.01	0.00
82	1309	2	−17	0.99	0.01	0.00
90	1418	−3	−52	0.96	0.04	0.00
91	1463	2	−19	0.99	0.01	0.00
99	1536	12	−727	0.62	0.29	0.07
105	1660	3	−40	0.98	0.02	0.00

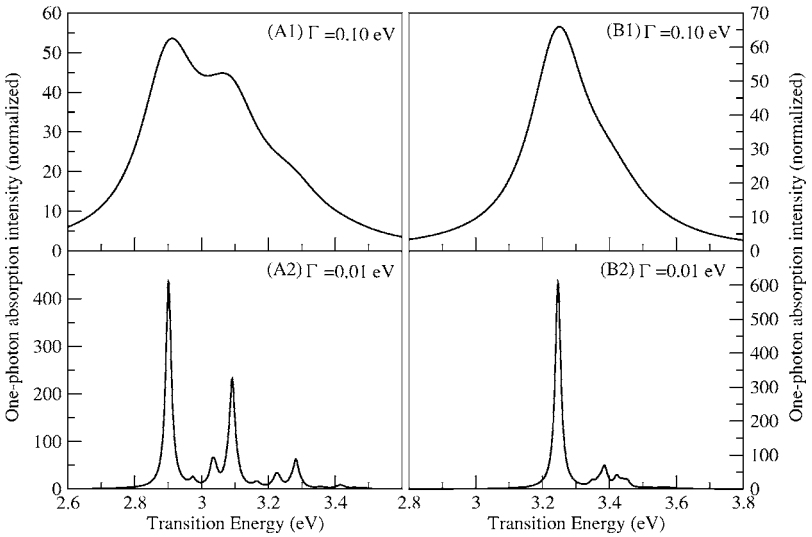

FIG. 5. Franck-Condon vibronic OPA spectrum of compound 1 in the DCM solution calculated with TD-B3LYP/PCM and B3LYP/PCM geometries (A1, A2) and with TD-B3LYP at B3LYP geometries (B1, B2). The lifetime broadenings of 0.1 and 0.01 eV are assumed.

Out of the 123 vibrational modes of compound 1, only less than 20 modes show considerable energy shifting. One can find that the 0-0 integral is always close to the value 1, except for mode 99 which has the largest energy shift with respect to the vertical transition. The vibration levels higher than 2 can be safely neglected. Most of the modes listed in Table II are related to the C–C stretching in the molecular back bond. Mode 69 is an exception which involves two O–B bonds connecting to the molecular back bond.

With the lifetime broadening of 0.01 eV, more vibronic fine structures can be resolved. As shown in Fig. 3 (A2), the highest peak at 2.90 eV is mainly from the 0-0 transition, while the second highest peak at 3.09 eV comes mainly from the 0-1 transition of mode 99, which is a C–C stretching mode in the molecular main axis with a frequency of 1536 cm^{-1} (0.19 eV). A small contribution from mode 90 with a frequency of 1418 cm^{-1} (0.17 eV) is also presented. The smaller peak at about 3.04 eV is mainly due to the 0-1 transition of mode 70 with a vibrational frequency of 1123 cm^{-1} (0.14 eV) and mode 69 with a vibrational frequency of 1059cm^{-1} (0.13 eV). The 0-2 transition of mode 99 results in another small peak at about 3.28 eV.

The solvent effect on the vibronic profile is clearly demonstrated in Fig. 5, in which the B3LYP results with and without solvent effects for the strong OPA state of compound 1 are presented. It should be reminded that the strong OPA state obtained from B3LYP for the gas phase is the S_2 state. Its spectral maximum is located at around 3.25 eV, which is 0.35 eV higher than the experimental result. Furthermore, the calculated vibronic profile from B3LYP for the gas phase shows no obvious structures.

It is interesting to examine the performance of HF for the vibronic profiles. The calculated results for compound 1 in the gas phase and in the DCM solution are shown in Fig. 6. The solvent effect on the vibronic profile is noticeable. It reduced the relative contribution of the second peak. Although the obtained absolute energy is about 1.3 eV too high, the overall spectral profile obtained at the HF level with the inclusion of solvent effect fits the experiment reasonably well.

IV. SUMMARY

It is, to the best of our knowledge, the first time that the solvent-induced vibronic profile of the one-photon absorption spectrum of a polyatomic organic molecule has been

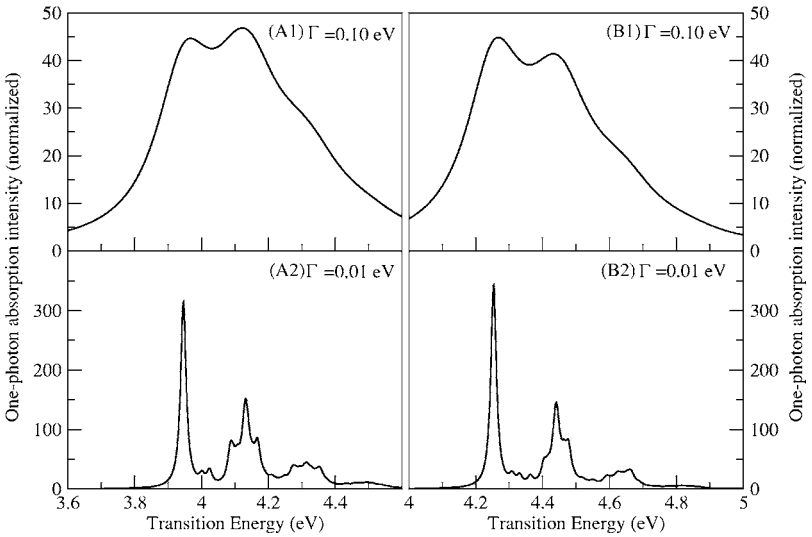

FIG. 6. Franck-Condon vibronic OPA spectra of compound 1 in DCM solution calculated with the TD-HF/PCM method at the HF/PCM geometry (A1, A2) and with the TD-HF method at the HF geometry (B1, B2). The lifetime broadenings are assumed to be 0.10 and 0.01 eV, respectively.

studied using the first-principles methods. We have also presented a useful computational scheme that can be easily adopted for similar studies.

We have calculated the vibronic profiles of the one-photon absorption spectra of compound 1 in the gas phase and in the DCM solution. Both the Franck-Condon and Herzberg-Teller contributions to the spectra are analyzed. It is found that several typical DFT methods fail to provide the correct description for the HOMO of compound 1 in the gas phase. With the inclusion of the solvent effect, the B3LYP method reproduces the spectral profile of the experimental OPA spectrum for compound 1 in the DCM solution. These phenomena might be useful for researchers who are interested in the performance of the DFT functionals. The vibronic profile of the OPA is dominated by the Franck-Condon contribution. The maximum of the Herzberg-Teller profile of the first excited state shows an interesting blueshift with respect to that of the Franck-Condon profile, which seems to explain the experimentally observed difference between spectral profiles of one- and two-photon absorptions of compound 1 in the DCM solution. The vibrational analysis reveals that the C–C stretching modes contribute the most to the vibronic profile.

[1] M. Albota, D. Beljonne, J.-L. Brédas *et al.*, Science **281**, 1653 (1998).
[2] M. Rumi, J. E. Ehrlich, A. A. Heikal *et al.*, J. Am. Chem. Soc. **122**, 9500 (2000).
[3] S. J. K. Pond, M. Rumi, M. D. Levin, T. C. Parker, D. Beljonne, M. W. Day, J. L. Brédas, S. R. Marder, and J. W. Perry, J. Phys. Chem. A **106**(47), 11470 (2002).
[4] S. Kato, T. Matsumoto, T. Ishi-i, T. Thiemann, M. Shigeiwa, H. Gorohmaru, S. Maeda, Y. Yamashita, and S. Mataka, Chem. Commun. (Cambridge) **20**, 2342 (2004).
[5] J.-D. Guo, C.-K. Wang, Y. Luo, and H. Ågren, Phys. Chem. Chem. Phys. **5**, 3869 (2003).
[6] C.-K. Wang, K. Zhao, Y. Su, Y. Ren, X. Zhao, and Y. Luo, J. Chem. Phys. **119**, 1208 (2003).
[7] I. Deperasinska, and J. Prochorow, Adv. Mol. Relax. Interact. Processes **11**, 51 (1977).
[8] J. E. Rogers, J. E. Slagle, D. G. McLean, R. L. Sutherland, B. Sankaran, R. Kannan, L. S. Tan and P. A. Fleitz, J. Phys. Chem. A **108**, 5514 (2004).
[9] J. A. Marsden, J. J. Miller, L. D. Shirtcliff, and M. M.Haley, J. Am. Chem. Soc. **127**, 2464 (2005).
[10] X.-H. Duan, X.-Y. Li, R.-X. He, and X.-M. Cheng, J. Chem. Phys. **122**, 084314 (2005).
[11] G. Nandini and D. N. Sathyanarayana, Spectrochim. Acta, Part A **60**, 1115 (2004).
[12] C. M. Previtali, Pure Appl. Chem. **67**, 127 (1995).
[13] J. Gierschner, H.-G. Mack, L. Lüer, and D. Oelkrug, J. Chem. Phys. **116**, 8596 (2002).
[14] J. Gierschner, H.-G. Mack, H.-J. Egelhaaf, S. Schweizer, B. Doser, and D. Oelkrug, Synth. Met. **138**, 311 (2003).
[15] M. Dierksen and S. Grimme, J. Chem. Phys. **120**, 3544 (2004).
[16] P. Macak, Y. Luo, and H. Ågren, Chem. Phys. Lett. **330**, 447 (2000).
[17] P. Rapta and H. Hartmann, Electrochim. Acta **39**, 2251 (1994).
[18] H.-D. Ilge, J. Photochem. **32**, 177 (1986).
[19] G. Goerlitz, Ber. Bunsenges. Phys. Chem. **102**, 1449 (1998).
[20] H. Hartmann, J. Prakt. Chem. **328**, 755 (1986).
[21] M. T. Cancs, B. Mennucci, and J. Tomasi, J. Chem. Phys. **107**, 3032 (1997); M. Cossi, V. Barone, B. Mennucci, and J. Tomasi, Chem. Phys. Lett. **286**, 253 (1998).
[22] J. B. Foresman, M. Head-Gordon, J. A. Pople, and M. J. Frisch, J. Phys. Chem. **96**, 135 (1992).
[23] E. Negri and M. Z. Zgierski, J. Chem. Phys. **100**, 2571 (1994).
[24] A. Dreuw, J. L. Weisman, and M. Head-Gordon, J. Chem. Phys. **119**, 2943 (2003).
[25] M. Dewar and W. Thiel, J. Am. Chem. Soc. **99**, 4499 (1977); L. P. Davis, R. M. Guidry, J. R. Williams, M. J. S. Dewar, and H. S. Rzepa, J. Comput. Chem. **2**, 433 (1981).
[26] A. D. Becke, Phys. Rev. A **38**, 3098 (1988).
[27] J. P. Perdew, Phys. Rev. B **33**, 8822 (1986).
[28] C. Lee, W. Yang, and R. G. Parr, Phys. Rev. B **37**, 785 (1988).
[29] A. D. Becke, J. Chem. Phys. **98**, 5648 (1993).
[30] G. A. Petersson and M. A. Al-Laham, J. Chem. Phys. **94**, 6081 (1991); G. A. Petersson, A. Bennett, T. G. Tensfeldt, M. A. Al-Laham, W. A. Shirley, and J. Mantzaris, *ibid.* **89**, 2193 (1988).
[31] M. J. Frisch, G. W. Trucks, H. B. Schlegel *et al.*, GAUSSIAN 03, revision B.03, Gaussian, Inc., Wallingford, CT, 2004.